Asian Journal of Chemistry Vol. 17, No. 3 (2005), 1863–1876

Ab initio Calculations and Rate Constant for the Reaction H + H_2

MARYAM DEHESTANI* and FAHIEMA SHOJAIE
Department of Chemistry
Shahid Bahonar University, P.O. Box 76169-133, Kerman, Iran
E-mail: dehestani2002@yahoo.com

Different levels of *ab initio* theory are used to calculate geometries, vibrational frequencies and energies for stationary points on the H + H_2 → H_2 + H reaction. Frequencies and geometries calculated for H_2 at the QCISD/cc-PVTZ and QCISD/aug-cc-PVTZ levels of theory are in very good agreement with experiment. The *ab initio* frequencies and geometries for the transition state are similar to those for the Liu-Siegbahn-Truhlar-Horowitz and double many-body expansion surfaces. Based on these *ab initio* calculations, thermal rate constants are calculated for the reaction H + H_2 → H_2 + H using the conventional transition state theory, thermodynamic formulation of transition state theory and semi-classical transition state theory.

Key Words: *Ab initio* calculation, Transition state theory, Semi-classical transition state theory.

INTRODUCTION

The potential energy surfaces (PES) for the collinear H + H_2 reaction have been studied from various view-points by many authors. There have been many semi-empirical, and *ab initio* approaches to compute a potential energy surface for this reaction[1, 2]. Most notable and accurate among the *ab initio* efforts are those by Liu and Siegbahn[3–5]. An analytical fit has been given by Truhlar and Horowitz[6]; therefore the PES is commonly referred to as the LSTH surface. There is another surface, which utilizes a double many body expansion technique and is called the double many body expansion (DMBE) surface[7]. More recently, density functional theory potential energy surfaces have been determined for this reaction, using the various hybrid exchange-correlation energy functionals[8].

The first aim of the present study is to perform geometry optimization, harmonic vibrational frequency, barrier height calculation for the H + H_2 reaction, by using up to date density functional calculation with a large set of basis set functions.

The H + H_2 reaction has been extensively studied over several decades, because it is the simplest bimolecular reaction and has always been of fundamental importance and considerable interest in the theory of chemical kinetics. This reaction has long been a testing ground for the comparison of theory and experiment. Due to many advances in both, the importance of this reaction has increased in recent years.

The early experimental data on the kinetics of the $H + H_2$ (v = 0) reaction were reported by Farkas[9]. Consistent thermal rate constants, k(T), for this reaction and its isotopic analogues, have been investigated as experimental by Le Roy and co-workers[10]. The experimental rate constant $H + H_2$ (v = 1) and deuterated isotopic variants of the reaction were measured using different techniques until 1985[11-13]. Theoretical developments have been carried out since the 1930's using potential energy surface[14-16] to describe nuclear motion during reaction and the transition state theory[17, 18] for calculation of rate constants. The method of quassiclassical trajectories (QCT) has been used to describe dynamic $H + H_2$ (v = 0) reaction by Porter and Karplus[1, 19] as well as this method was used in the case of the reaction with H_2 (v = 1) by Mayne and Toennies[20]. The calculation of quantum mechanic (QM) on empirical potential energy surfaces of Porter and Karplus[1] has been performed and given cross sections and thermal rate constants for the $H + H_2$ reaction by Kuppermann and co-workers[21, 22]. Transition state theory was used to calculate k(T) for this reaction on the Liu-Siegbahn-Truhlar-Horowitz potential energy surfaces (LSTH PES)[23]. To improve the conventional transition state theory, Garrett and co-workers[23-25] applied the canonical variational transition state theory (VTST) with introduction tunneling corrections to obtain accurate results for the $H + H_2$ (v = 0) reaction on the LSTH PES, $H + H_2$ (v = 1) and $D + H_2$ (v = 1) reactions[25, 26]. Several approximate quantum dynamical methods were used to calculate the rate constants for these reactions[27, 28]. Different kinds of semi-classical approximation were used to evaluate quantum mechanical transition state theory expression and applied their numerical results for the collinear $H + H_2$ and isotopic variations[29-31].

The second purpose of this paper is to perform the conventional transition state theory (CTST), thermodynamic formulation of transition state theory (TFTST) and semi-classical transition state theory (SCTST) introduced by Miller and coworkers[30] to calculate the thermal rate constants of the reaction $H + H_2$ using a potential energy surface fitted to our best *ab initio* calculations.

Theory

Different methods have been proposed to calculate thermal rate constant. The following three methods were chosen:

Conventional Transition State Theory

One of the most useful descriptions of chemical reaction rates is transition state theory which was developed in the 1930's by Pelzer and Wigner, Evans and Polanyi, and Eyring[32]. This theory provides the most useful approxi- mation for obtaining the rate of bimolecular reactions. Conventional transition state theory is explained in many text books. We have considered this theory with statistical factor and tunneling effect as a specifically quantum phenomenon.

The transition state theory rate constant with tunneling correction for bimolecular reaction $A + BC \rightarrow AB + C$ is given by

$$k = \Gamma \frac{k_B T}{h} \frac{Q^{\pm}}{Q_A Q_{BC}} \exp\left(-\frac{E_0}{K_B T}\right) \tag{1}$$

where k_B, T, h and E_0 are Boltzmann constant, temperature, Planck constant and quantum barrier height respectively. The ratio k_BT/h is called the frequency factor because of having the units of frequency. $Q^{\pm}$, Q_A and Q_{BC} are complete transition-rotation-vibration-electronic partition functions of the activated complex and reactants, respectively. Γ is one-dimensional tunneling correction and this correction appears to be important for reactions involving very light species, such as H or D atoms. Several methods have been proposed to calculate tunneling corrections for transition state theory reaction rates[33]. In the simplest form, the barrier is taken to be an inverse harmonic oscillator or an Eckart barrier. In this work, the Eckart correction is used to account for quantum mechanical tunneling and is given by[34]

$$\Gamma = 1 - \frac{1}{24}\left(\frac{h\nu_F}{k_B T}\right)^2 \left(1 + \frac{k_B T}{E_0}\right) \tag{2}$$

where ν_F is imaginary frequency of activated complex.

The rate constant with statistical factor can be written by[35]

$$k = L^{\pm} \frac{k_B T}{h} \frac{Q^{\pm}}{Q_A Q_{BC}} \exp\left(-\frac{E_0}{K_B T}\right) \tag{3}$$

If all identical atoms in a reaction are labelled, so that they distinguish from another, in this case the number of different transition states that can be formed is called statistical factor ($L^{\pm}$). This factor is 2 for forming the transition state of the $H + H_2$ reaction.

Thermodynamic formulation of transition state theory

The transition state derived rate constant can be reformulated in thermodynamic terms the molar Gibbs standard free energy ($\Delta G_0^{\pm}$), standard enthalpy and entropy changes as

$$k = \Gamma \frac{k_B T}{h} e^{\Delta S_0^{\pm}/R} e^{-\Delta H_0^{\pm}/RT} \tag{4}$$

The expression of rate constant with statistical factor is same as in above equation except k(T) including $L^{\pm}$ instead of Γ.

Semi-classical transition state theory

The thermal rate constant for a bimolecular reaction, such as $A + BC \rightarrow AB + C$, can be written as[29, 36]

$$k^{j=0}(T) = (2\pi\hbar\ Q_r)^{-1}\int_0^\infty dE \exp\left(-\frac{E}{k_BT}\right)N^{j=0}(E) \qquad (5)$$

where N(E) and Q_r are the cumulative reaction probability (CRP) and partition function (per unit volume) for reactants, respectively.

The CRP is given by

$$\{N(E) = \sum_{n_1}\ldots \sum_{n_{F-1}}\ldots P_{n_1}, n_{F-1}(E) \qquad (6)$$

where $P_{n_1}, \ldots n_{F-1}$ is tunnelling probability for state $\underline{n} = (n_1 \Lambda\, n_{F-1})$ of activated complex with the total energy E.

For a transition state with F degrees of freedom in which motion along a reaction coordinate (the Fth degree of freedom) is separable from F – 1 others, and in the semi-classical approximation, transmission probability of activated complex can be written as

$$P_{n_1,\ldots n_{F-1}}(E) = [1 + e^{2\theta P_{n_1,\ldots n_{F-1}}, E)}]^{-1} \qquad (7)$$

where $\theta(P_{n_1,\ldots n_{F-1}}E)$ is the action integral through the barrier and in the harmonic approximation is[30]

$$\theta(\{P_{n_1,\ldots n_{F-1}}, E) = \frac{\pi\left(\sum_{k}^{F-1}\omega_k\left(n_k + \frac{1}{2}\right) + \sum_{s}\omega_s(n_s + 1) - E + V_0\right)}{\overline{\omega}_F} \qquad (8)$$

where V_0 is the potential energy at the saddle point, ω_k and ω_s are the non-degenerate and doubly degenerate harmonic modes frequencies for F – 1 vibrational normal modes of activated complex, respectively, and $\overline{\omega}_F$ is reactive mode frequency. Note that the potential along the reaction coordinate (mode F) is a harmonic barrier so that the frequency $\overline{\omega}_F$ is imaginary.

Computational procedures

The hybrid density functional B3LYP, Moller-Plesset correlation energy correction MP2, quadratic configuration interaction method (QCISD), coupled cluster doubles method (CCD), couper cluster singles and doubles method (CCSD) and configuration interaction double method (CID) to account for electron correlation effects have been used. Geometry optimization and harmonic vibrational frequencies of H_2 and H_3 were calculated by these methods using the 6-31+G*, 6-311G**, cc-PVDZ, cc-PVTZ, aug-cc-PVDZ and aug-cc-PVTZ basis sets. These calculations were performed employing the Gaussian 98 suite of programs[37].

RESULTS AND DISCUSSION

The calculated bond lengths, vibrational frequencies and electronic energies for H_2 molecule and transition state (H_3) in different levels and basis sets, are listed in Tables 1–3. As shown in Tables 1 and 2, the geometries and *ab initio* harmonic frequencies for H_2 calculated at the level QCISD with cc-PVTZ and aug-cc-PVTZ basis sets, are in very good agreement with the experimental structure ($R_{HH} = 0.74$ Å) and harmonic vibrational frequency ($\omega = 4401$ cm^{-1}). As seen in Tables 1–3, in the transition state, at the level QCISD with basis sets cc-PVTZ and aug-cc-PVTZ, bond length and vibrational frequencies and classical barrier height are in very good agreement with results of LSTH and DMBE surfaces. Present *ab initio* calculations at this level with basis sets cc-PVTZ and aug-cc-PVTZ of the H_3 potential energy surface give a linear transition state with the same band distances $R_{HH} = 0.9301$ and 0.9313 Å, classical reaction barriers (*i.e.*, energy of the transition state with respect to the minimum of the isolated H_2 potential) of 10.27 and 10.05 kcal/mol, respectively. LSTH and DMBE found the bond lengths and classical reaction barriers at transition state to be 0.9298 and 0.9238 Å, 9.80 and 9.65 kcal/mol, respectively. Since the level QCISD with basis sets cc-PVTZ and aug-cc-PVTZ can provide perfect results in geometries, vibrational frequencies and barrier height, they are employed to calculate rate constant of the H + H_2 reaction.

TABLE-1

AB INITIO MINIMUM-ENERGY GEOMETRIES

Basis set Level		6-31+G**	6-311G**	cc-PVDZ	cc-PVTZ	aug-cc-PVDZ	aug-cc-PVTZ
HF	H_2	0.7346	0.7384	0.7480	0.7344	0.7481	0.7344
	TS	0.9158	0.9187	0.9323	0.9180	0.9328	0.9189
MP2	H_2	0.7338	0.7384	0.7544	0.7369	0.7549	0.7374
	TS	0.9158	0.9187	0.9323	0.9180	0.9328	0.9189
B3LYP	H_2	0.7428	0.7442	0.7617	0.7429	0.7608	0.7429
	TS	0.9315	0.9312	0.9464	0.9304	0.9442	0.9301
CID	H_2	0.7377	0.7429	0.7602	0.7421	0.7611	0.7425
	TS	0.9197	0.9233	0.9372	0.9243	0.9388	0.9255
QCISD	H_2	0.7462	0.7435	0.7609	0.7426	0.7617	0.7432
	TS	0.9414	0.9291	0.9432	0.9301	0.9449	0.9313
CCD	H_2	0.7457	0.7429	0.7602	0.4721	0.7608	0.7424
	TS	0.9197	0.9233	0.9372	0.9243	0.9388	0.9255
CCSD	H_2	0.7384	0.7435	0.7609	0.7426	0.76168	0.7429
	TS	$R_1 = 1.1579$	$R_1 = 0.9999$	$R_1 = 0.8412$	$R_1 = 1.0000$	$R_1 = 1.1587$	$R_1 = 1.0587$
		$R_2 = 0.9251$	$R_2 = 0.9290$	$R_2 = 0.9427$	$R_2 = 0.9300$	$R_2 = 0.9442$	$R_2 = 0.9342$

Distances are in angstroms. Bond angle (H, X, H) is 90 degree and dihedral angle (H, X, H, H) is 180 degree in all levels for transition state. The experimental bond distance for H_2 is 0.74 Å, bond distance for H_3 at the LSTH and DMBE surfaces are 0.9298 and 0.9238 Å respectively.

TABLE-2

AB INITIO VIBRATIONAL FREQUENCIES[a]

Basis set / Level		6-31+G**	6-311G**	cc-PVDZ	CC-PVTZ	aug-cc-PVDZ	aug-cc-PVTZ
HF	H_2	4635.1000	4526.1321	4583.9118	4587.3759	3235.9427	4585.7841
	ω_1	2051.5299	2048.7104	2045.9275	2035.7390	2035.4225	2035.6346
	ω_2	1005.9232	987.9731	916.0361	913.8849	889.4350	897.6873
	$\overline{\omega}_4$	2357.3536	2347.3987	2273.4748	2298.1592	2266.4529	2297.3249
MP2	H_2	4609.2212	4533.2235	4501.2609	4526.3627	4463.6879	4517.6448
	ω_1	2137.1150	2152.6777	2161.8618	2151.0098	2138.1177	2143.2674
	ω_2	1037.7557	973.6807	933.5992	929.4925	916.4531	896.2607
	$\overline{\omega}_4$	2108.4001	1994.0148	1973.7982	1968.3421	1944.9851	1965.8592
B3LYP	H_2	4465.6534	4419.2512	4368.3720	4419.6822	4356.1846	4417.4247
	ω_1	2079.1712	2056.9022	2062.6002	2056.8556	2052.9232	2056.5956
	ω_2	992.5566	943.4976	906.0655	923.4567	9321.9183	914.8856
	$\overline{\omega}_4$	824.8174	746.2334	529.4902	756.0293	551.0405	744.3502
CID	H_2	4519.6589	4434.5355	4398.9979	4422.0066	4359.1159	4412.6211
	ω_1	2137.8551	2117.7264	2134.4080	2110.1538	2104.1626	2100.2219
	ω_2	1016.6191	957.2087	918.8305	922.2738	896.8981	886.9385
	$\overline{\omega}_4$	1895.3915	1741.7072	1686.7332	1709.8132	1654.8124	1709.9944
CCSD	H_2	4504.8047	4420.7814	4382.1979	4410.6655	4345.1104	4401.7441
	ω_1	2084.0487	2061.2098	2076.2090	2052.0473	2046.8071	2040.9823
	ω_2	1009.7795	952.6252	911.3862	917.6319	888.9402	883.6031
	$\overline{\omega}_4$	1739.0015	1571.5890	1493.7365	1538.4950	1461.1043	1538.9051
CCD	H_2	4519.6596	4434.5364	4397.8791	4422.0074	4362.4046	4414.1814
	ω_1	2137.8542	2117.7169	2134.4067	2110.1533	2104.1616	2100.9989
	ω_2	1016.6195	957.2105	918.8314	922.2748	896.8931	886.9395
	$\overline{\omega}_4$	1895.3893	1741.7136	1686.7338	1709.8153	1654.8126	1706.9989
QCISD	H_2	4504.1338	4420.1286	4382.5584	4409.3876	4344.4990	4401.1477
	ω_1	2085.0973	2061.5753	2074.0787	2053.0532	2043.9580	2043.3164
	ω_2	1009.4411	951.9870	913.4813	917.1152	891.6390	882.2965
	$\overline{\omega}_4$	1734.1241	1566.5337	1497.8502	1531.9370	1467.2406	1531.9990

[a] The harmonic frequencies are in units of cm^{-1}. ω_1 = frequencies of symmetric stretch, ω_2 = frequencies of degenerate bend, $\overline{\omega}_4$ = frequencies of the imaginary reaction mode. The experimental vibrational frequency for H_2 is 4401 cm^{-1}, the harmonic frequencies for H_3 at the LSTH surface are $\omega_1 = 2059$, $\omega_2 = 910$, $\overline{\omega}_4 = 1506$ and at the DMBE surface are $\omega_1 = 2066.9$, $\omega_2 = 899.5$, $\overline{\omega}_4 = 493.1$ cm^{-1}.

The present *ab initio* calculations as well as three methods discussed in section of theory were employed to calculate rate constant of the $H + H_2$ reaction. First, we have performed calculations using CTST method with Eckart tunnelling and with statistical factor for the rate constant $H + H_2 \rightarrow H_2 + H$ reaction. From *ab initio* calculation results, complete transition-rotation-vibration-electronic partition functions of the activated complex (H_3), reactants (H_2 and H) and tunnelling correction were calculated, then the rate constants were calculated *via* Eq. (1) with tunnelling effect and Eq. (3) with statistical effect ($L^{\pm} = 2$) at each temperature. The comparison between these results with the results of other works and two sets of experimental values is represented in Table-4.

TABLE-3
AB INITIO ENERGIES

Level \ Basis set		6-31+G**	6-311G**	cc-PVDZ	CC-PVTZ	aug-cc-PVDZ	aug-cc-PVTZ
HF	$H_2 + H^a$	1.629501	1.634523	1.628061	1.632783	1.628101	1.763284
	TS^a	1.601007	1.610526	1.601141	1.604799	1.601440	1.604865
	E_0^b	17.880290	15.078220	16.861840	17.578250	16.761430	17.591650
	E_0^c	17.096430	14.173540	15.852840	16.543420	15.697730	16.512850
MP2	$H_2 + H^a$	1.655894	1.660082	1.654496	1.664459	1.655551	1.664844
	TS^a	1.636007	1.642326	1.638051	1.647990	1.640127	1.648651
	E_0^b	12.479290	11.142060	10.319400	10.334650	9.678463	10.161640
	E_0^c	11.963470	10.523440	9.644201	9.596071	9.057228	9.329567
BELYP	$H_2 + H^a$	1.678812	1.681686	1.674860	1.682155	1.675682	1.682279
	TS^a	1.672244	1.674932	1.669843	1.675388	1.670652	1.675532
	E_0^b	4.121235	4.238071	3.148217	4.245791	3.156249	4.233935
	E_0^c	3.547941	3.558474	2.713335	3.531056	2.531249	3.474648
CID	$H_2 + H^a$	1.663191	1.667976	1.662808	1.672009	1.664111	1.672332
	TS^a	1.640919	1.648398	1.644566	1.654098	1.644566	1.654763
	E_0^b	13.975900	12.285070	11.446910	11.239430	12.264330	11.024660
	E_0^c	13.477030	11.709650	10.836340	10.571220	11.710280	10.254710
CCSD	$H_2 + H^a$	1.663390	1.668150	1.662951	1.672145	1.664233	1.672457
	TS^a	1.642516	1.650062	1.646212	1.655739	1.648966	1.656442
	E_0^b	13.098200	11.350460	10.498870	10.294920	9.580195	10.065260
	E_0^c	11.080760	9.339294	8.505270	9.548063	7.564437	8.049260
CCD	$H_2 + H^a$	1.663191	1.667976	1.662807	1.672008	1.664110	1.672332
	TS^a	1.640919	1.648398	1.644566	1.565409	1.647305	1.654763
	E_0^b	13.975840	12.285070	11.446220	11.238640	10.545310	11.024530
	E_0^c	13.476970	11.709650	10.835630	10.570340	9.831199	10.252690
QCISD	$H_2 + H^a$	1.663390	1.668150	1.662951	1.672146	1.664233	1.672445
	TS^a	1.642541	1.650091	1.646240	1.655777	1.648998	1.656443
	E_0^b	13.082950	11.332260	10.485790	10.271710	9.559989	10.048750
	E_0^c	12.511290	10.682160	9.786744	9.525601	8.820789	9.200363

[a] The electronic energies are in units hartrees (negative).

[b] The classical reaction energies do not include zero-point energies are in kcal mol^{-1}.

[c] The quantum reaction energies include zero-point energies are in kcal mol^{-1}.

As seen in Table-4, the CTST k(T) with tunnelling correct from *ab initio* calculations at QCISD level and basis set aug-cc-PVTZ agree with results of Garrett *et al.*[25], Park and Light[38], Colton and Schatz[39] and the experimental data[40, 41] at low temperatures. However, since the tunnelling effect is not important at high temperatures, CTST including this correct cannot reproduce the good results for temperatures larger than 440 K. The agreement between quantum rate constants and the CTST results with statistical factor is better than the ones with tunnelling effect at high temperatures.

TABLE-4

COMPARISON OF CTST RATE CONSTANT (cm^3 $molecule^{-1}$ s^{-1}) OF THIS WORK WITH OTHER RESULTS AND THE EXPERIMENT

T (K)	k(T)[38]	k(T)[39]	k(T)[25]	k(T)[b] exp	k(T) QCISD[c]	k(T) QCISD[d]	k(T) QCISD[e]	k(T) QCISD[f]
299	2.56 (−16)[a]	1.6 (−16)	2.2 (−16)	2.7(−16), 2.6(−16)	1.508 (−16)	8.868 (−17)	1.805 (−16)	1.060 (−16)
300	2.76 (−16)	1.7 (−16)	2.3 (−16)	—	1.575 (−16)	9.303 (−17)	1.884 (−16)	1.112 (−16)
327	7.49 (−16)	4.4 (−16)	5.5 (−16)	5.4 (−16), 5.2 (−16)	4.568 (−16)	3.025 (−16)	5.378 (−16)	3.559 (−16)
346	1.412 (−15)	8.0 (−16)	9.8 (−16)	9.8 (−16), 8.3 (−16)	8.696 (−16)	6.185 (−16)	1.014 (−15)	7.207 (−16)
440	1.42 (−14)	7.7 (−15)	8.8 (−15)	9.4 (−15), 7.1 (−15)	8.826 (−15)	8.240 (−15)	9.912 (−15)	9.248 (−15)
500	3.7 (−14)	2.3 (−14)	—	—	2.377 (−14)	2.509 (−14)	2.623 (−14)	2.767 (−14)
600	1.27 (−13)	8.7 (−14)	9.3 (−14)	—	7.627 (−14)	9.389 (−14)	8.276 (−14)	1.012 (−13)
700	3.48 (−13)	—	—	—	1.708 (−13)	2.316 (−13)	1.811 (−13)	2.454 (−13)
900	1.25 (−12)	—	—	—	4.624 (−13)	7.122 (−13)	4.787 (−13)	7.370 (−13)
1000	2.03 (−12)	1.7 (−12)	1.7 (−12)	—	6.376 (−13)	1.023 (−12)	6.544 (−13)	1.049 (−12)

[a] 2.56(−16) = 2.56 × 10^{-16}.

[b] The results obtained from Refs. [40, 41].

[c, d] This work is in basis set cc-PVTZ with tunnelling correction and statistical factor, respectively.

[e, f] This work is in basis set aug-cc-PVTZ with tunnelling correction and statistical factor, respectively.

Then to obtain thermal rate constants for this reaction using TFTST with Eckart tunnelling and with statistical factor, it was necessary to have thermodynamic function of transition state. The *ab initio* calculations were used to determine the standard enthalpy and entropy changes at each temperature. Of these properties, the rate constants were calculated using Eq. (4) at different temperatures and compared with the quantum results[38, 43] in Table-5. Since, the agreement between the quantum rate constants and TFTST k(T) at QCISD/aug-cc-PVTZ with statistical factor are good at high temperatures, we can assume that the obtained thermodynamic functions from our *ab initio* calculations are accurate for these temperatures. Our results for both tunnelling effect and statistical factor, however, are in poor agreement with quantum ones at the low temperatures lower than 500 K, where tunnelling is important. Thus, it seems clear that our *ab initio* calculations give a low quality prediction for the thermodynamic function, as well as the ultra simple Eckart correction used in our calculation is not adequate at low temperatures.

TABLE-5

COMPARISON OF TFTST THERMAL RATE CONSTANT (cm^3 molecule^{-1} s^{-1}) OF THIS WORK WITH OTHER WORKS

T (K)	k(T)[38]	k(T)[43]	k(T) QCISD[a]	k(T) QCISD[b]	k(T) QCISD[c]	k(T) QCISD[d]
300	1.171(–17)	8.505 (–18)	1.183 (–18)	6.987 (–19)	2.871 (–18)	1.695 (–18)
400	1.802 (–16)	1.291 (–16)	3.074 (–17)	2.594 (–17)	8.378 (–17)	7.068 (–17)
500	9.480 (–16)	—	2.082 (–16)	2.197 (–16)	4.248 (–16)	4.483 (–16)
600	2.829 (–15)	1.988 (–15)	7.396 (–16)	9.051 (–16)	1.407 (–15)	1.721 (–15)
700	6.077 (–15)	4.250 (–15)	1.836 (–15)	2.488 (–15)	3.471 (–15)	4.710 (–15)
800	1.063 (–14)	—	2.979 (–15)	5.341 (–15)	5.371 (–15)	7.836 (–15)
900	1.621 (–14)	—	6.317 (–15)	9.729 (–15)	1.182 (–14)	1.821 (–14)
1000	2.250 (–14)	1.578 (–14)	9.856 (–15)	1.582 (–14)	1.421 (–14)	2.281 (–14)

[a, b] This work is in basis set cc-PVTZ with tunnelling correction and statistical factor, respectively.

[c, d] This work is in basis set aug-cc-PVTZ with tunneling correction and statistical factor, respectively.

Finally, thermal rate constants for zero total angular momentum were calculated between 300 and 1000 K using SCTST. We have calculated the rate constants by Eqs. (5)–(8) using described method[30]. The integral in Eq. (5) was evaluated using a four point Gauss-Legendre quadrature with 500 quadrature points. Table-6 compares the rate constants using SCTST method from present *ab initio* calculation results and three of quantum thermal rate constants[38, 42, 43] and the semi-classical ones of Miller *et al.*[30] using both harmonic and anharmonic constants. At high temperature, where anharmonic effects are less important, *e.g.*, in the range between 700 and 1000 K, the SCTST thermal rate constants from our *ab initio* calculations using harmonic effects were found to be in close agreement with the quantum calculations and the harmonic and anharmonic versions of the semi-classical theory (Table-6), but our results deviate gradually from those with decreasing temperature, and at 300 K these results are about one-half of the quantum ones.

TABLE-6

COMPARISON OF SCTST THERMAL RATE CONSTANT (cm^3 $molecule^{-1}$ s^{-1})OF THIS WORK WITH OTHER RESULTS

T(K)	k(T)[38a]	k(T)[42a]	k(T)[43a]	k(T)[30b]	k(T)[30c]	k(T) QCISD[d]	k(T) QCISD[e]
300	1.171 (–17)	—	8.505 (–18)	—	—	3.98 (–18)	6.309 (–18)
400	1.802 (–16)	—	1.291 (–16)	—	—	7.586 (–17)	1.005 (–16)
500	9.480 (–16)	1.071 (–15)	—	—	—	4.467 (–16)	5.623 (–16)
600	2.829 (–15)	—	1.988 (–15)	1.944 (–15)	2.032 (–15)	1.445 (–15)	1.718 (–15)
700	6.077 (–15)	6.422 (–15)	4.250 (–15)	—	—	3.707 (–15)	3.839 (–15)
800	1.063 (–14)	—	—	—	—	7.447 (–15)	7.721 (–15)
900	1.621 (–14)	1.663 (–14)	—	—	—	1.288 (–14)	1.371 (–14)
1000	2.250 (–14)	—	1.578 (–14)	1.864 (–14)	1.817 (–14)	2.138 (–14)	1.862 (–14)

[a]Quantum results, [b]anharmonic results, [c]harmonic results,[d, e] thiswork. This work is in basis set cc-PVTZ and basis set aug-cc-PVTZ, respectively.

The respective rate constants, k (T; v = 0, j = 0), CTST, TFTST with tunnelling correction and with statistical factor and SCTST, are depicted as a function of the inverse of the temperature in the Figs. 1 and 2 at the level QCISD with basis set cc-PVTZ and in Figs. 3 and 4 with basis set aug-cc-PVTZ, respectively, and are

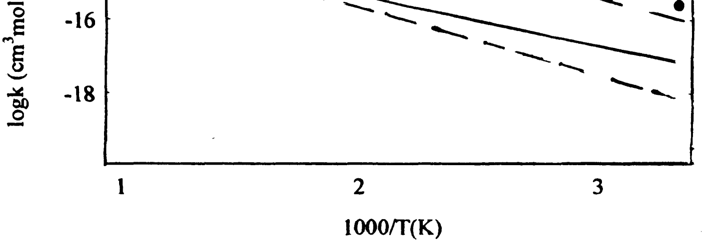

Fig. 1. Comparison of calculated and experimental rate constants for $H + H_2$ the collinear reaction. The points are the experimental results obtained from Ref. [40]. The solid, dashed and dot-dashed lines are the results of SCTST, CTST and TFTST calculations with tunneling correction, respectively. These calculations are in the QCISD/cc-PVTZ

compared with experimental values[40]. Figs. 1 and 3 show that CTST with tunnelling can explain the experimental results at low temperature. Comparing Fig. 2 with Fig. 4, we can see that when a statistical factor is applied to a conventional transition state, the correlation of experiment and theory is good, except at low temperatures. This substantiate the fact that a tunneling correction should be applied in conventional transition state theory at low temperatures and a statistical factor at high temperatures where tunnelling is not important. There are significant differences in the calculated rate constants using TFTST and SCTST methods with experimental and CTST results. The TFTST and SCTST k(T) calculated with our *ab initio* calculations are systematically lower than CTST ones and the experimental values. As shown in Figs 1–4, the rate constants obtained with QCISD level and basis sets cc-PVTZ and aug-cc-PVTZ are not

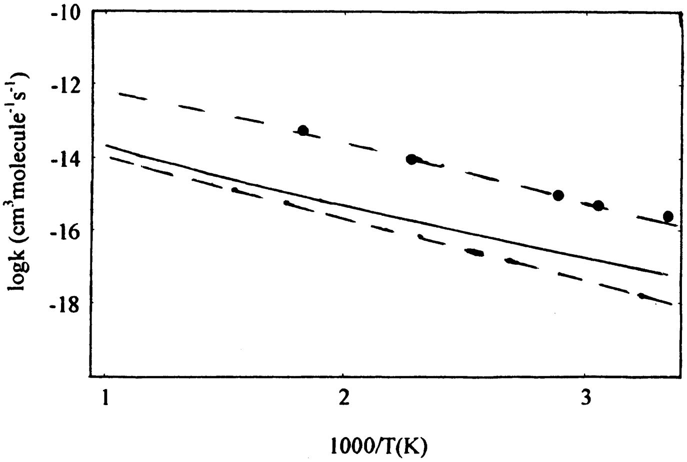

Fig. 2. Same as Fig. 1 except TFTST and CTST calculations with statistical factor

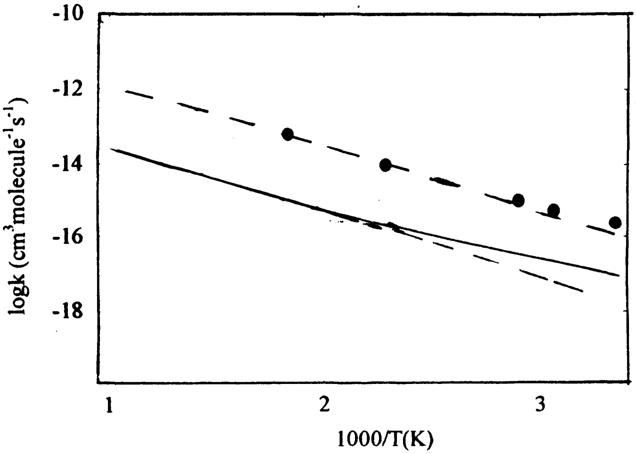

Fig. 3. Same as Fig. 1 except in the QCISD/aug-cc-PVTZ

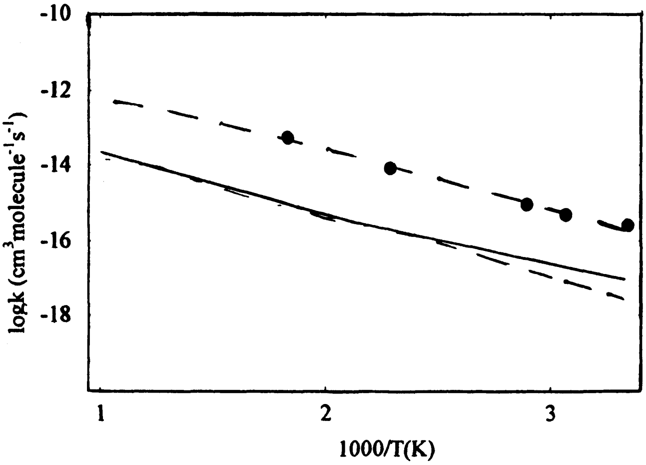

Fig. 4. Same as Fig. 2 except in the QCISD/aug-cc-PVTZ

quite similar to each other. The QCISD level with basis set aug-cc-PVTZ gives better results in rate constants compared to the QCISD level with basis set cc-PVTZ, so that the best accord between CTST rate constants and experiment is obtained at this level with basis set aug-cc-PVTZ.

In our calculations all frequencies were taken as harmonic. Since the anharmonic effect on the reactive and transition state partition functions is small, CTST k(T) with tunnelling at low temperatures, and with statistical factor at high temperatures is reliable. Harmonic version of the SCTST theory fails to predict the rate constants at low temperature. Therefore, it seems that accounting for modes anharmonicity may be important for reactions involving the transfer of light atoms at low temperature, where anharmonic effects are important.

Conclusion

Ab initio calculations have been carried out in order to determine the best level and basis sets for potential energy surface of reaction $H + H_2$. The level QCISD with basis sets cc-PVTZ and aug-cc-PVTZ give the most accurate geometries for reactant (H_2) and a similar geometry for the transition state (H_3). These *ab initio* calculations for the $H + H_2$ reaction, which is presumed to have accurate geometries, harmonic frequencies and barrier height, is applied to calculate rate constant of this reaction. Three methods, the CTST, TFTST with Eckart tunnelling and with statistical factor and SCTST of Miller have been used to calculate the thermal rate constant reaction $H + H_2$ from our *ab initio* calculations. The comparison of CTST results with the available experimental values reveals a good agreement with tunnelling effect at low temperatures and with statistical factor at high temperatures.

REFERENCES

1. R.N. Porter and M. Karplus, *J. Chem. Phys.*, **40**, 1105 (1964).
2. E. Edmiston and M. Krauss, *J. Chem. Phys.*, **42**, 192 (1968); D. G. Truhlar and R. E. Wyatt, *Adv. Chem. Phys.*, **36**, 141 (1977).
3. B. Liu, *J. Chem. Phys.*, **58**, 1925 (1973).
4. P. Siegbahn and B. Liu, *J. Chem. Phys.*, **68**, 2457 (1978).
5. B. Liu (1977) private communication.
6. D.G. Truhlar and C.J. Horowitz, *J. Chem. Phys.*, **68**, 2466 (1978).
7. A.J.C. Varandas, F.B. Brown, C.A. Mead, D.G. Truhlar and N.C. Blais, *J. Chem. Ph* 6258 (1987).
8. D.M. Grant, P.J. Wilson, D.J. Tozer and S.C. Althorpe, *Chem. Phys. Lett.*, **375**, 162 (2003).
9. (a) A. Farkas, *Z. Phys. Chem.*, **10**, 419 (1930); (b) A. Farkas and L. Farkas, *Proc. R. Soc. London*, **152A**, 124 (1935).
10. D.N. Mitchell and D.J. LeRoy, *J. Chem. Phys.*, **58**, 3449 (1973) and references therein.
11. E.B. Gordon, B.I. Ivanov, A.P. Perminov, V.G. Balalaev, A. Ponomarev and V. Filatov, *Chem. Phys. Lett.*, **58**, 425 (1978) and references therein.
12. G.P. Glass and B.K. Chaturvedi, *J. Chem. Phys.*, **77**, 3478 (1982).
13. U. Wellhausen and J. Wolfrum, *J. Ber. Bunsen-Ges. Phys. Chem.*, **89**, 316 (1985) and references therein.
14. F. London, *Z. Electrochem.*, **35**, 552 (1929).
15. H. Eyring and M. Polanyi, *Z. Phys. Chem., B*, **12**, 279 (1931).
16. H. Pelzerand and E. Wigner, *Z. Phys. Chem., B*, **15**, 445 (1932).
17. M.G. Evans and M. Polanyi, *Trans. Faraday Soc.*, **31**, 857 (1935).
18. H. Eyring, *J. Chem. Phys.*, **3**, 107 (1935).
19. R.N. Porter and M. Karplus, *Discuss. Faraday Soc.*, **44**, 164 (1967).
20. H.R. Mayne and J.P. Toennies, *J. Chem. Phys.*, **75**, 1794 (1981).
21. A. Kuppermann, G.C. Schatz and M. Baer, *J. Chem. Phys.*, **65**, 4596 (1976).
22. G.C. Schatz and A. Kuppermann, *J. Chem. Phys.*, **75**, 1794 (1981).
23. B.C. Garrett and D.G. Truhlar, *J. Chem. Phys.*, **72**, 3460 (1980).
24. ————, *Proc. Natl. Acad. Sci. USA*, **76**, 4755 (1979).
25. B.C. Garrett, D.G. Truhlar, A.J.C. Varandas and N.C. Blais, *Int. J. Chem. Kinet.*, **18**, 1065 (1986).
26. B.C. Garrett and D.G. Truhlar, *J. Phys. Chem.*, **89**, 2204 (1985).
27. R. B. Walker and E. Pollak, *J. Chem. Phys.*, **83**, 2851 (1985).
28. E. Pollak, N. Abu Salbi and N. Kouri, *J. Chem. Phys. Lett.*, **113**, 585 (1985).
29. S. Chapman, B.C. Garrett and W.H. Miller, *J. Chem. Phys.*, **63**, 2710 (1975).
30. M.J. Cohen, N.C. Handy, R. Hernandez and W.H. Miller, *J. Chem. Phys. Lett.*, **192**, 407 (1992).
31. T. Yamamoto and W.H. Miller, *J. Chem. Phys.*, **118**, 2135 (2003).
32. K.J. Laidler and M.C. King, *J. Phys. Chem.*, **87**, 2657 (1983).
33. B.C. Garrett and D.G. Truhlar, *J. Phys. Chem.*, **83**, 200 (1979); *J. Chem. Phys.*, **79**, 4931 (1983).
34. C. Eckart, *Phys. Rev.*, **35**, 1303 (1930).
35. J.I. Steinfeld, J.S. Francisco and W.L. Hase, Chemical Kinetics and Dynamics, Prentice-Hall International, New York (1989).
36. W.H. Miller, *J. Chem. Phys.*, **62**, 1899 (1975).
37. M.J. Frisch, G.W. Trucks, H.B. Schlegel, G.E. Scuseria, M.A. Robb, J.R. Cheeseman, V.G.

Zakrzewski, J.A. Montgomery, Jr., R.E. Stratmann, J.C. Burant, S. Dapprich, J.M. Millam, A.D. Daniels, K.. Kudin, M.C. Strain, O. Farkas, J. Tomasi, V. Barone, M. Cossi, R. Cammi, B. Mennucci, C. Pomelli, C. Adamo, S. Clifford, J. Ochterski, G.A. petersson, P.Y. Ayala, Q. Cui, K. Morokuma, D.K. Malick, A.D. Rabuck, K. Raghavachari, J.B. Foresman, J. Cioslowski, J.V. Ortiz, A.G. Baboul, B.B. Stefanov, G. Liu, A. Liashenko, P. Piskorz, I. Komaromi, R. Gomperts, R.L. Martin, D.J. Fox, T. Keith, M.A. Al-Laham, C.Y. Peng, A. Nanayakkara, C. Gonzalez, M. Challacombe, P.M.W. Gill, B. Johnson, W. Chen, M.W. Wong, J.L. Andres, C. Gonzalez, M. Head-Gordon, E.S. Replogle and J.A. Pople, GAUSSIAN 98, Revision A. 7. Gaussian Inc., Pittsburgh, PA (1998).

38. T.J. Park and J.C. Light, *J. Chem. Phys.*, **91**, 974 (1989).
39. M.C. Colton and G.C. Schatz, *Int. J. Chem. Kinet.*, **18**, 961 (1986).
40. T. Yamamoto, *J. Chem. Phys.*, **33**, 281 (1960).
41. T.J. Park and J.C. Light, *J. Chem. Phys.*, **88**, 4897 (1988).
42. F. Webster and J.C. Light, *J. Chem. Phys.*, **90**, 265 (1989).
43. D.C. Chatfield, D.G. Truhlar and D.W. Schwenke, *J. Chem. Phys.*, **94**, 2040 (1991).

(*Received*: 20 October 2004; *Accepted:* 16 April 2005) AJC-4181